J. Fluid Mech. (1970), *vol.* 41, *part* 3, *pp.* 509–521
Printed in Great Britain

Waves on a stream of finite depth which has a velocity defect near the free surface

By P. L. BETTS
Department of Mechanical Engineering, University of Manchester Institute of Science and Technology

(Received 23 December 1968 and in revised form 21 October 1969)

The conditions under which stationary waves may exist on a stream of water of finite depth are investigated theoretically for the case of a current which is uniform except for a constant defect in velocity in a region near the free surface. The analysis is extended to provide a two-dimensional theory for the surface profile induced by a simplified model of a hovering craft. The relevance of this work to the use of high speed flumes is discussed, and an example demonstrates the importance of the velocity distribution near the free surface.

1. Introduction

The present interest in hovering and hydrofoil craft as a means of transport over water has lead to the development of a number of high-speed circulating water channels, notably at the Universities of Leeds and Liverpool. In such a channel, the water issues from a fully enclosed contraction into a working section where it has a free surface. Binnie, Davies & Orkney (1955) noted that, unless special precautions are taken, a boundary layer is shed from the lid of the contraction, and there is a noticeable defect in velocity near the free surface throughout the working section.

A channel of this type would not be used for conventional ship resistance tests, and so the interest is wholly in the effect that the surface wake might have on water waves. Taylor (1955), in his work on the hydraulic breakwater, derived the theoretical results for free waves advancing into and being stopped by an opposing surface current above an otherwise stationary sea. A simple change in co-ordinates, to a set moving with the waves, leads directly to a method for calculating the wavelength of the stationary waves that may appear on the surface of a current which is uniform except close to the free surface. Taylor's analysis can be applied equally well to the case of a defect in velocity at the free surface as to an excess, although he only made numerical calculations relevant to the latter. However, his theory only applies to a stream of infinite depth and, since the channels discussed can be run at velocities corresponding to Froude numbers (main stream velocity$/(g \times \text{depth})^{\frac{1}{2}}$) of up to two, it seems desirable to investigate the situation further for depths which are not large compared with the length of the stationary waves.

The theoretical approach in the present paper differs from that of Taylor in that a frame of reference is taken which is stationary relative to the wave train (i.e. stationary relative to any model placed in the channel), and also the problem is approached by considering the application of a spatially periodic, but time independent, pressure to the free surface. In this way, not only can the condition for stationary waves be determined (corresponding to zero amplitude of pressure fluctuation), but also a two-dimensional theory can be derived for the effect of the surface wake on the disturbance caused by a simplified hovering craft.

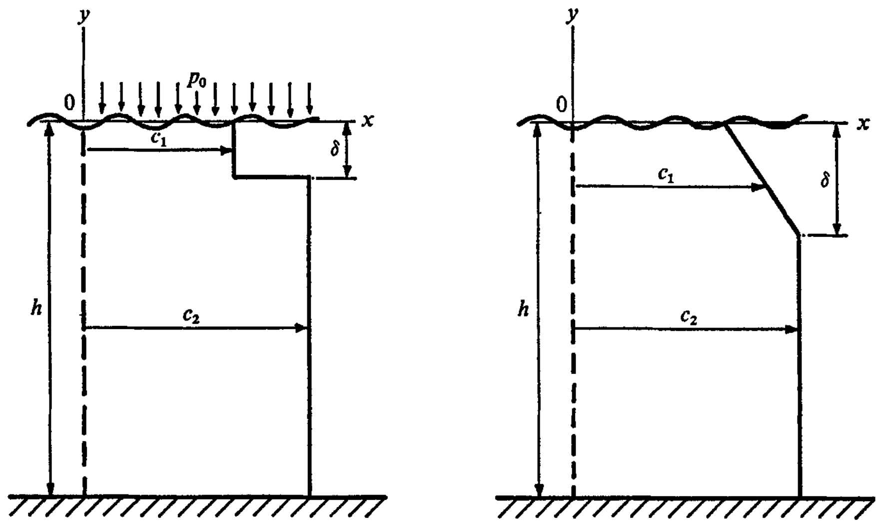

FIGURE 1. Assumed distribution of velocity in surface wakes.

2. The effect of a spatially periodic pressure applied to the free surface

Take as co-ordinates x, horizontal and positive in the direction of the underlying current, and y vertical and positive upwards, the origin being in the undisturbed free surface (figure 1 (a)). Let the undisturbed velocity of the underlying current be c_2 and that within the surface wake c_1; both of which are independent of y. The total depth of water is denoted by h, the depth of the velocity defect region by δ, and the pressure imposed on the free surface by $p_0 = C \cos kx$. A velocity distribution such as that shown in figure 1 (a) would be impossible in practice, since it is highly unstable at the velocity discontinuity and would soon develop into one more like that shown in figure 1 (b). However, Taylor's work shows that the major features of surface waves on the two velocity distributions are the same when h is infinite, and only the case of a uniform velocity defect will be considered here.

The analysis is similar to that of Lamb (1932, Art. 245) where he considers the effect of a spatially periodic pressure on a uniform stream (i.e. $c_1 = c_2$ or $\delta = 0$). When viscosity is neglected, Laplace's equation is satisfied in each region, and we can assume that the stream function is given by

$$\psi/c_1 = -y + (\alpha_1 \sinh ky + \beta_1 \cosh ky) \cos kx, \tag{2.1a}$$

and

$$\psi/c_2 = -y + (\alpha_2 \sinh ky + \beta_2 \cosh ky) \cos kx + A \tag{2.1b}$$

within the wake and the underlying main stream respectively, where A is a constant.

At the bottom, $y = -h$,

$$\partial\psi/\partial x = -kc_2(-\alpha_2 \sinh kh + \beta_2 \cosh kh) \sin kx = 0,$$

or
$$\psi/c_2 = -y + \gamma_2 \sinh k(y+h) \cos kx + A \tag{2.2}$$

in the main stream, where

$$\gamma_2 = \alpha_2/\cosh kh = \beta_2/\sinh kh.$$

The interface between the two currents is a common streamline at, say, $y = -\delta + \epsilon \cos kx$, and hence

$$\begin{aligned} c_1(\delta - \epsilon \cos kx) + c_1[\alpha_1 \sinh k(-\delta + \epsilon \cos kx) + \beta_1 \cosh k(-\delta + \epsilon \cos kx)] \cos kx \\ = c_2(\delta - \epsilon \cos kx) + c_2\gamma_2 \sinh k(h - \delta + \epsilon \cos kx) \cos kx + c_2 A \\ = \text{constant}. \end{aligned}$$

Equating the fluctuating parts of each expression to zero, and ignoring terms of order ϵ^2, leads to

$$\begin{aligned} \epsilon &= -\alpha_1 \sinh k\delta + \beta_1 \cosh k\delta \\ &= \gamma_2 \sinh k(h-\delta). \end{aligned} \tag{2.3}$$

The requirement that the static pressure should be continuous across the interface yields the further condition

$$c_1^2(\alpha_1 \cosh k\delta - \beta_1 \sinh k\delta) = c_2^2 \gamma_2 \cosh k(h-\delta), \tag{2.4}$$

when second-order terms are again neglected.

The linearized conditions at the free surface are

$$y = \beta_1 \cos kx, \tag{2.5}$$

from (2.1a) and
$$\frac{p_0}{\rho} = \frac{C \cos kx}{\rho} = -gy + kc_1^2 \alpha_1 \cos kx,$$

from the pressure condition. Thus,

$$C/\rho = kc_1^2 \alpha_1 - g\beta_1. \tag{2.6}$$

When α_1 and γ_2 are eliminated from (2.3), (2.4) and (2.6), the resulting equation for the wave amplitude β_1 is

$$C/\rho = \beta_1 c_1^2 (kF - k_2), \tag{2.7}$$

where
$$F = \frac{c_2^2 \coth k(h-\delta) \coth k\delta + c_1^2}{c_2^2 \coth k(h-\delta) + c_1^2 \coth k\delta}$$

and
$$k_2 = g/c_1^2.$$

The form of the free surface is then given by

$$y = \frac{C \cos kx}{\rho c_1^2 (kF - k_2)}. \tag{2.8}$$

3. The condition for free stationary waves

If the pressure over the free surface is uniform, $C = 0$ and stationary waves (of amplitude $\beta_1 \neq 0$) are only possible if

$$\frac{kc_1^2[c_2^2 \coth k(h-\delta)\coth k\delta + c_1^2]}{c_2^2 \coth k(h-\delta) + c_1^2 \coth k\delta} - g = 0. \tag{3.1}$$

This equation determines the wavelength $(2\pi/k)$ of possible stationary waves on the given stream. It is convenient to express (3.1) in non-dimensional form. This may be accomplished in several ways. The one followed here is to take

$$R = \frac{\delta}{h}, \quad V = \frac{c_1}{c_2}, \quad T = k\delta, \quad U = \frac{kc_2^2}{g}. \tag{3.2}$$

Equation (3.1) is then

$$U = \frac{1}{V^2}\left\{\frac{\coth T[(1/R)-1] + V^2 \coth T}{\coth T[(1/R)-1]\coth T + V^2}\right\}. \tag{3.3}$$

The results of interest are values of T for given values of R, V, and either $c_2/(g\delta)^{\frac{1}{2}} (\equiv [U/T]^{\frac{1}{2}})$ or $c_2/(gh)^{\frac{1}{2}}$ $(\equiv [UR/T]^{\frac{1}{2}})$. Some numerical computations of (3.3) are displayed in figures 2 and 3.

In figure 2, where T is plotted against $(U/T)^{\frac{1}{2}}$, the limit $R \to 0$ corresponds to $h \to \infty$, and equation (3.3) reduces, with a change in terminology, to Taylor's hydraulic breakwater equation.† In figure 3, where T/R $(\equiv kh)$ is plotted against $(UR/T)^{\frac{1}{2}}$, the limit $R \to 0$ corresponds to $\delta \to 0$. In general, it appears that on both figures a change in V is more important than one in R. This effect is due to the physical importance of the velocity close to the free surface and is in agreement with a conclusion of Taylor's that a surface current of constant velocity in deep water will have the same stopping effect as one of the same thickness, but with constant vorticity, when the velocity of the former is somewhat greater than the average velocity of the latter.

A value of V greater than unity has been included on both the figures as this would correspond to an over enthusiastic use of boundary-layer injection at the trailing edge of the contraction lid, and injection is a possible method for eliminating the velocity defect. A velocity ratio V more than unity corresponds, with a change in reference frame, to the case of a hydraulic breakwater, but the stopping effect on waves below a certain wavelength is not immediately obvious because of the way in which the figures have been plotted.

The maximum value of $(UR/T)^{\frac{1}{2}}$ for which waves can exist on the flow occurs when $k \to 0$. Multiplication of both the numerator and denominator in (3.1) by $\tanh k(h-\delta) \tanh k\delta$ and taking the limit as $k \to 0$ leads to the equation

$$\left(\frac{UR}{T}\right)^{\frac{1}{2}} = \frac{c_2}{(gh)^{\frac{1}{2}}} = \left[1 + R\left(\frac{1}{V^2} - 1\right)\right]^{\frac{1}{2}}. \tag{3.4}$$

† Scales of $c_1/(g\delta)^{\frac{1}{2}} \equiv (UV^2/T)^{\frac{1}{2}}$ are also shown in figure 2. Since the disturbance caused by the waves is negligible beyond $\frac{1}{2}\lambda$ below the free surface, the effect of the underlying current is negligible when $\delta/\lambda \equiv T/2\pi > 0{\cdot}5$. In this region, all the curves in figure 2 collapse to a single curve when plotted as T against $c_1/(g\delta)^{\frac{1}{2}}$. Similarly, the value of the depth h has negligible effect when $h/\lambda \equiv T/2\pi R > 0{\cdot}5$.

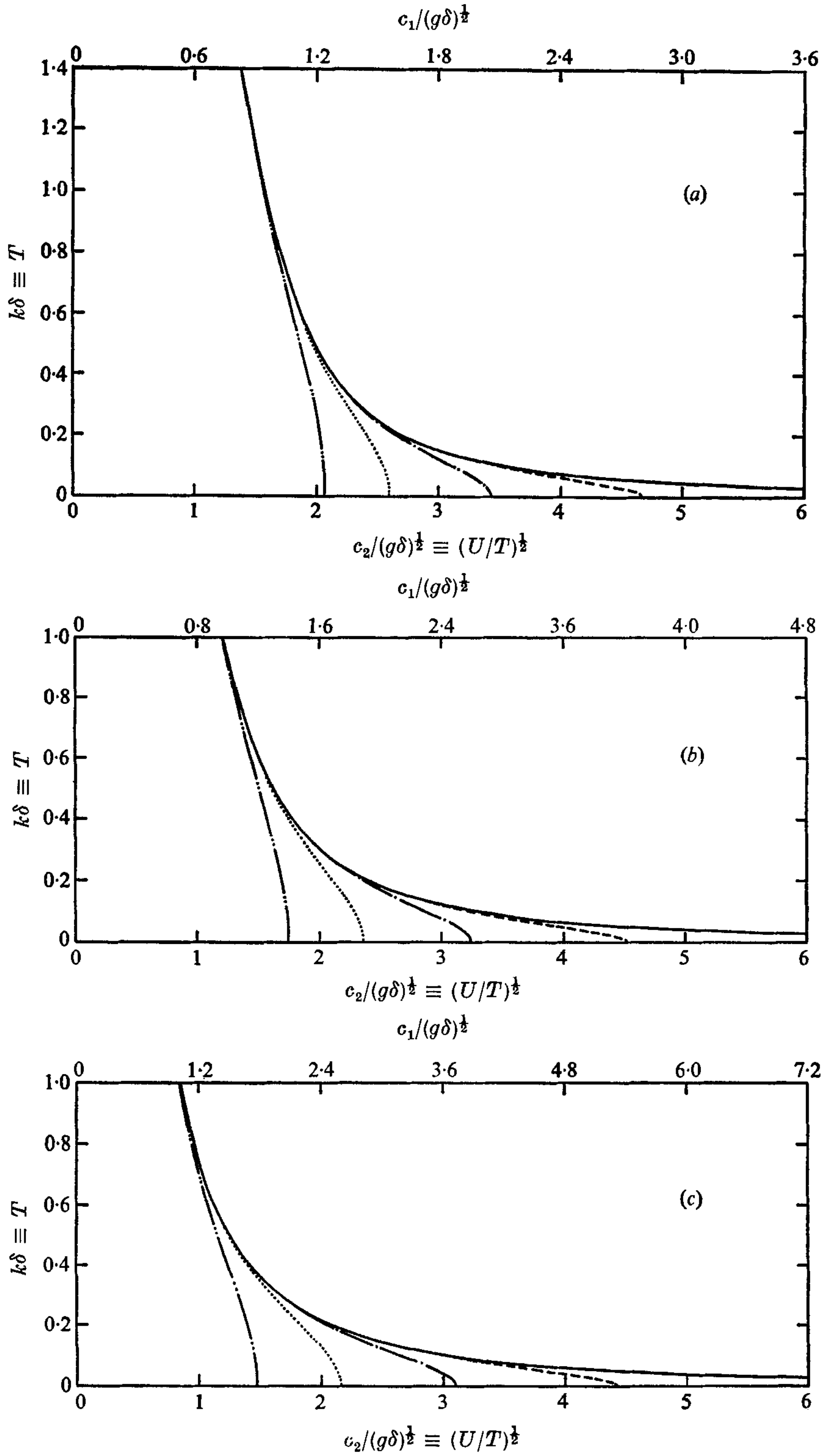

FIGURE 2. The effect on the wave-number of free stationary waves as the depth $h \rightarrow \infty$: (a) $V \equiv c_1/c_2 = 0{\cdot}60$; (b) $V = 0{\cdot}80$; (c) $V = 1{\cdot}20$; ———, $R \equiv \delta/h = 0$; – – – –, $R = 0{\cdot}05$; –·–·—·—, $R = 0{\cdot}10$; . . . . , $R = 0{\cdot}20$; —··—··—, $R = 0{\cdot}40$.

Physically, this is the measured or nominal Froude number above which no waves of infinitesimal amplitude can exist.

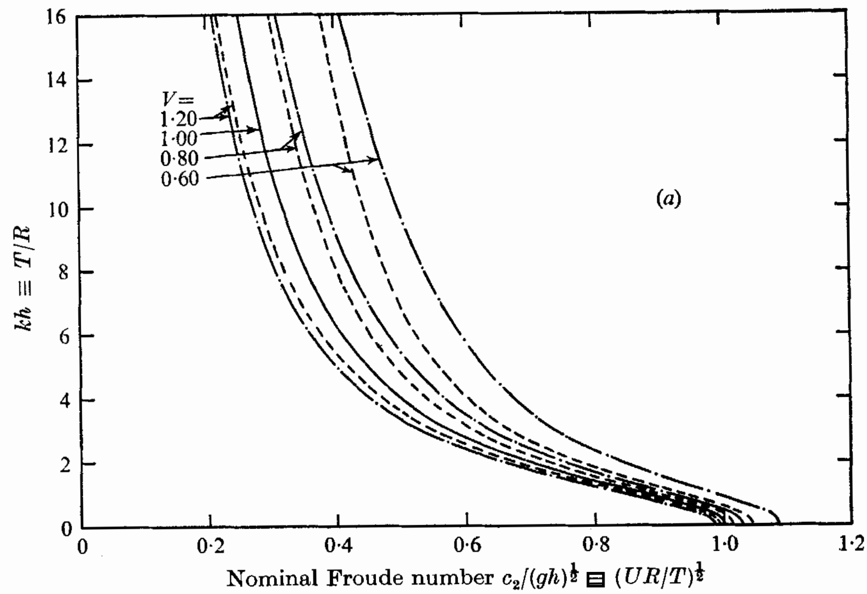

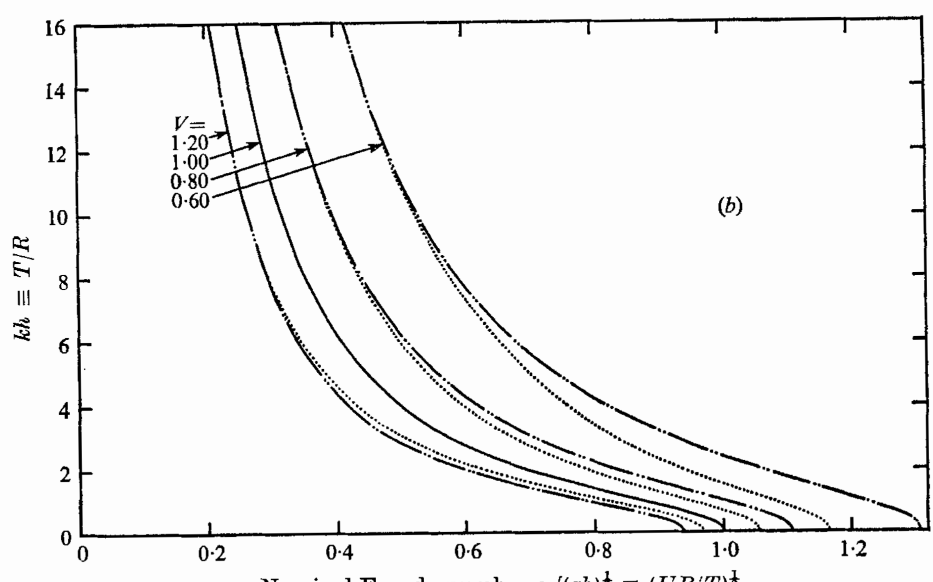

FIGURE 3. (*a*) and (*b*) The effect on the wave-number of free stationary waves as the thickness of the surface wake tends to zero. The values of V are stated on the figures: ———, $R \equiv \delta/h = 0$; – – – –, $R = 0{\cdot}05$; —·—·—, $R = 0{\cdot}10$; ...., $R = 0{\cdot}20$; —··—··—, $R = 0{\cdot}40$.

4. The surface profile caused by a simplified model of a hovering craft

The solution expressed by (2.8) may be generalized to construct the effect of an arbitrary distribution of pressure, say

$$p_0 = p(x), \tag{4.1}$$

with the aid of Fourier's double-integral theorem. Lamb (1932, Art. 245) has derived the surface form of a uniform stream with a band of pressure imposed on it such that $p(x)$ equals zero for all but infinitesimal values of x, for which it becomes infinite in such a way that

$$\int_{-\infty}^{\infty} p(x)\,dx = P. \tag{4.2}$$

This gives the effect of a finite force P per unit length across the flow concentrated on an infinitely narrow band of the surface at the origin. It may therefore be considered as a first approximation to a hovering craft, which completely spans the flow and has a length short in comparison to that of the surface waves (cf. Hogben 1967).

Generalizing (2.8) in the same way gives

$$y = \frac{P}{\pi\rho c_1^2}\int_0^{\infty} \frac{\cos kx}{kF - k_2}\,dk \tag{4.3}$$

as the representation of the effect of the pressure distribution defined by (4.1) and (4.2) on a stream with a surface wake. Equation (4.3) may be written as

$$\frac{\pi\rho c_1^2 y}{P} = \int_0^{\infty} \frac{\cos(Tx/\delta)}{T.F(T) - k_2\delta}\,dT, \tag{4.4}$$

where T, R and V are the dimensionless groups defined in equations (3.2), and

$$F(T) = \frac{\coth T[(1/R)-1]\coth T + V^2}{\coth T[(1/R)-1] + V^2 \coth T}.$$

The integral in (4.4) can be evaluated by contour integration in a manner similar to that used by Lamb. As in the case with a uniform stream, the complex function of $\zeta(\equiv T + iT_i)$ under the integral sign has a singular point at $\zeta = \mp i\infty$ according as x is positive or negative, and the remaining singular points are given by the zeros of the denominator, which are here roots of the equation

$$\zeta.F(\zeta) - k_2\delta = 0. \tag{4.5}$$

This equation is somewhat more complicated than the equivalent equation with a uniform stream, but since the Laplace equations for the stream function are of the Sturm–Liouville form, there can be no complex eigenvalues of k^2 in (3.1). Consequently the roots of (4.5) are still either real or pure imaginary.

When $c_1^2/g\delta > 1 + V^2[(1/R)-1]$, it follows from (3.4) that there are no real roots of (4.5) but only an infinite series of pure imaginary ones. For x positive, the surface profile is obtained by integrating around the upper half-plane and is given by

$$y = \frac{iP}{\rho c_1^2}\sum \frac{\exp(i\zeta_s x/\delta)}{f'(\zeta_s)}, \tag{4.6}$$

where ζ_s is a typical root of (4.5), the sum is taken over all the singularities in the upper half-plane, and

$$f'(\zeta) = F(\zeta) + \zeta . F'(\zeta).$$

Since ζ_s is always a positive imaginary number ($\zeta_s = i\eta_s$ say), each term in the summation decays exponentially as $\exp(-\eta_s x/\delta)$ with distance from the origin,

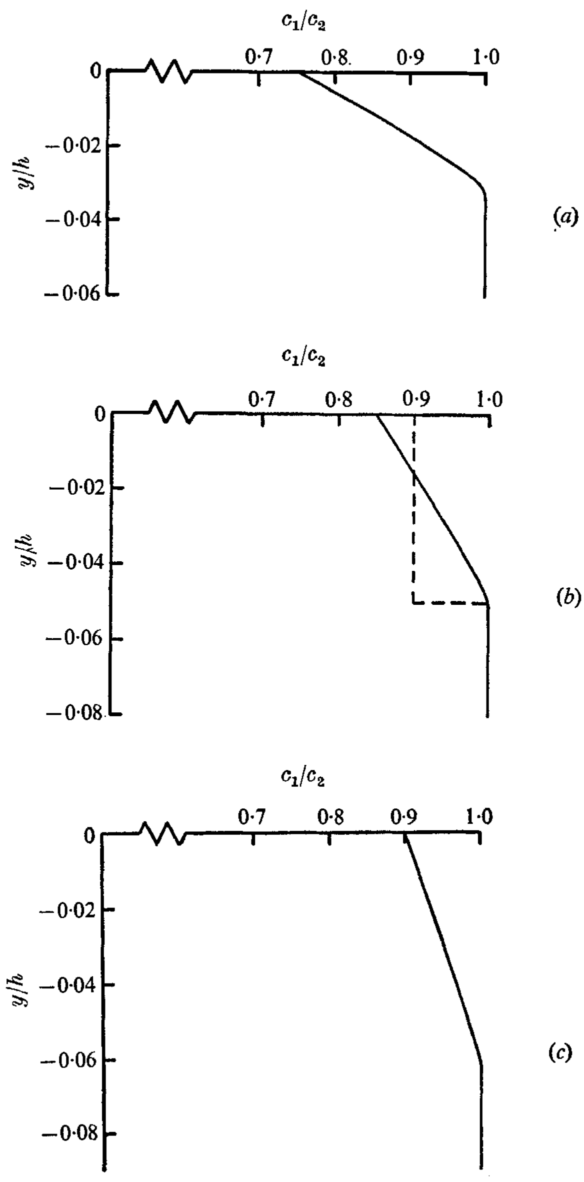

FIGURE 4. Comparison of assumed distribution of velocity in surface wake with experimental distribution measured in the Liverpool University high speed flume with $c_2 = 5$ ft./s and $h = 2{\cdot}75$ ft.: ———, experimental distribution; (a) immediately downstream of contraction; (b) in working section 6 ft. downstream; (c) 12 ft. downstream. – – – –, distribution assumed to be equivalent to the experimental distribution (b).

and the surface elevation, which is symmetrical about the band of pressure, tends to zero at large distances from it.

When $c_1^2/g\delta < 1+V^2[(1/R)-1]$, (4.5) has a pair of real roots ($\pm\xi$ say), and the lowest pair of pure imaginary roots has disappeared. The integral in (4.4) is then indeterminate and we are reduced to finding its Cauchy principal value. The required contour of integration is again similar to that used by Lamb, the points $\zeta = \pm\xi$ being excluded by small semi-circles, and the additional condition of wave free water upstream must be introduced. The surface form, for x positive, is then found to be

$$y = -\frac{2P}{\rho c_1^2}\frac{\sin(\xi x/\delta)}{f'(\xi)} + \frac{iP}{\rho c_1^2}\sum\frac{\exp(i\zeta_s x/\delta)}{f'(\zeta_s)}, \tag{4.7}$$

and for x negative

$$y = \frac{iP}{\rho c_1^2}\sum\frac{\exp(-i\zeta_s x/\delta)}{f'(\zeta_s)}. \tag{4.8}$$

The real roots $\pm\xi$ are, of course, not included in these summations over the singularities in the upper half-plane. The general form of the surface is therefore similar to that which would occur on a uniform stream, namely a local deformation, which is symmetrical about the band of pressure and negligible at large distances from it, added to a trailing stationary wave train of constant amplitude. The length of the waves $(2\pi\delta/\xi)$ is equal to that of the free stationary waves discussed in § 3, and the sine phase arises because the origin represents the complete hovering craft and not just the leading or trailing edge.

5. An example of practical interest

The velocity profiles shown on figure 4 were measured in the high-speed flume at Liverpool University before any attempts were made to reduce the surface wake. The uniform velocity defect profile, which is also shown on figure 4, may be taken as a reasonable approximation to the profile in the working section (cf. § 3). The value of $R = \delta/h$ is therefore 0·05 and $V = c_1/c_2 = 0{\cdot}90$, and we shall consider numerically the surface profiles induced by the band of pressure when the nominal Froude number of the stream $(c_2/(gh)^{\frac{1}{2}})$ is 0·5 and 2·0.

Consider the pure imaginary roots ($\zeta = i\eta$) given by (4.6). When η is large, the values of η approach the roots of

$$\frac{1-V^2\tan\eta[(1/R)-1]\tan\eta}{\tan\eta+V^2\tan\eta[(1/R)-1]} = 0 \tag{5.1}$$

from below. Moreover, since $[(1/R)-1] = 19$, which is an integer, the value of the function in (5.1) is repeated at intervals of π, and there are 20 roots within a range of π of η. Thus for any root $\zeta_s = i\eta_s$ of the full equation (4.5), there is another root $\zeta_{(s+20)} = i(\eta_s+\pi+\Delta)$, where Δ is small when η_s is large. Since $f'(\zeta_s)$ in (4.6) and (4.7) is always positive imaginary and $f'(\zeta_{(s+20)})$ is greater than $f'(\zeta_s)$, it is possible to put upper and lower bounds on the local elevations given in (4.6), (4.7) and (4.8).

For each value of x, the lower bound is obtained by simply curtailing the infinite series in the equations after a finite number of terms. The series was curtailed after the 93rd term for $c_2/(gh)^{\frac{1}{2}} = 0{\cdot}5$ and after the 94th term for $c_2/(gh)^{\frac{1}{2}} = 2{\cdot}0$. The difference in the number of terms is due to the disappearance of the lowest root at the lower Froude number. The upper bounds were obtained by summing the first 73 and 74 terms respectively and then adding to these values the sums of the 20 geometric progressions given by

$$\frac{iP}{\rho c_1^2 f'(i\eta_s)} \sum_{r=0}^{\infty} \exp\{-(\eta_s + r\pi)\,|x|/\delta\},$$

where $i\eta_s$ is a typical root of (4.5) included in the last 20 terms of the lower bound series. The differences between the upper and lower bounds of the local elevations were found to be negligible except at very small values of $|x|$. This region has

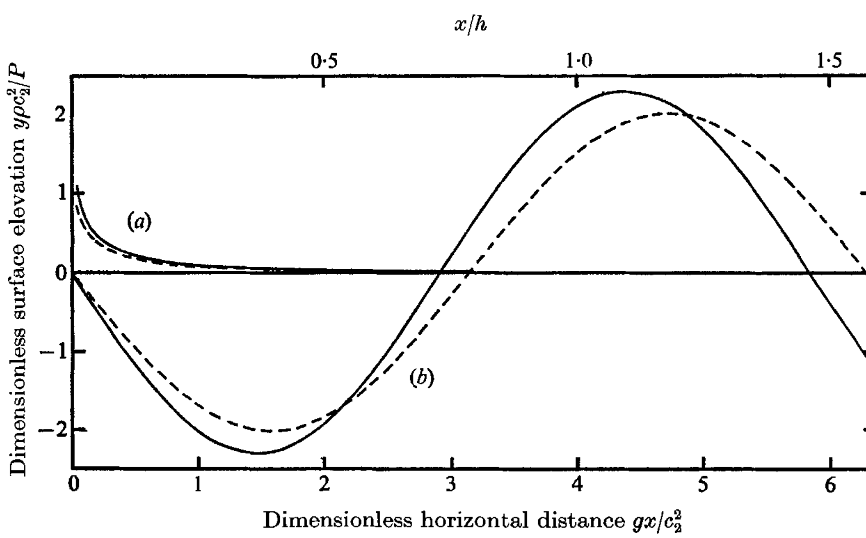

FIGURE 5. Components of surface profiles caused by band of pressure with $c_2/(gh)^{\frac{1}{2}} = 0{\cdot}5$; ———, with surface wake, $R = 0{\cdot}05$, $V = 0{\cdot}90$; – – – –, uniform stream: (*a*) local elevation profile; (*b*) trailing wave profile.

been omitted from the curves of local elevation shown in dimensionless form on figures 5 and 6, since it is also the region in which the artificiality of the pressure band and the effects of linearization will be most noticeable. The calculations of the wave component in (4.7) when $c_2/(gh)^{\frac{1}{2}} = 0{\cdot}5$ are straightforward, and the results are also shown on figure 5; the total elevation is therefore the sum of the two curves (*a*) and (*b*) on this figure.

For comparison, similar calculations have been performed for a uniform stream at Froude numbers of 0·5 and 2·0. The method of summing the infinite series was similar to that described above, except that only one geometric progression was needed. The first 99 and 100 terms respectively were used for the lower bounds. The results of these calculations are also shown on figures 5 and 6, and the effects of the surface wake are immediately apparent. The wake increases the amplitude of the trailing wave on figure 5 by 14 % and reduces its length by 7 %; to obtain a trailing wave with the same value of kh on a uniform stream would require a reduction in the Froude number of $3\frac{1}{2}$ %, even though the wake only reduces the average velocity of the stream by $\frac{1}{2}$ %. The percentage increase in the local elevation, caused by the velocity defect, at comparable values of both x/h and gx/c_2^2 is greater at the lower value of $c_2/(gh)^{\frac{1}{2}}$. Indeed, for $c_2/(gh)^{\frac{1}{2}} = 2{\cdot}0$ (figure 6), there is a small decrease in local elevation when $gx/c_2^2 > 0{\cdot}2$.

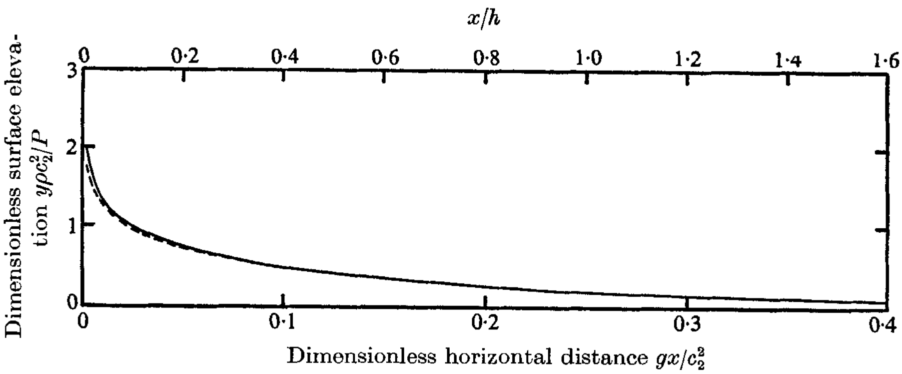

FIGURE 6. Surface profiles caused by band of pressure with $c_2/(gh)^{\frac{1}{2}} = 2{\cdot}0$; ———, with surface wake, $R = 0{\cdot}05$, $V = 0{\cdot}90$; – – – –, uniform stream.

Calculations have also been performed, at selected values of R and V, to determine the effect of the surface wake on the amplitude of the trailing waves over a range of Froude numbers. The results of these are displayed on figure 7 as values of the ratio of the amplitude (a_δ) with a surface wake to that (a) on a uniform stream of depth h and velocity c_2. The corresponding values of the wavelengths can be obtained from figure 3. The effect of the bottom on waves on the uniform stream is negligible for values of the Froude number, $c_2/(gh)^{\frac{1}{2}}$, less than about $\frac{1}{2}$, and consequently $a \propto 1/c_2^2$, since the model hovering craft is always in the high planing region because the band of pressure is infinitely short along the flow. As $c_2/(gh)^{\frac{1}{2}}$ is increased beyond $\frac{1}{2}$, the effect of the finite depth of the stream becomes increasingly important and the amplitude reaches a minimum value, after which it increases until it eventually tends to infinity as the Froude number approaches unity.

When there is a surface wake, the underlying current has a negligible effect on the waves when the wavelength is less than twice the wake thickness. Thus at low values of $c_2/(gh)^{\frac{1}{2}}$, $a_\delta \propto 1/c_1^2$, and consequently $a_\delta/a = 1/V^2$. As the Froude number increases, so does the wavelength; the initial effect of the underlying stream is to make the value of a_δ depart even further from that of a, but at slightly higher Froude numbers this effect is reversed. At high subundal Froude numbers, with $V < 1$, the rapidly increasing value of a starts to dominate the ratio a_δ/a until, at $c_2/(gh)^{\frac{1}{2}} = 1$, $a_\delta/a = 0$. Beyond this, values of a_δ exist, but there can be no waves on the superundal uniform stream. When $V > 1$, a_δ increases more rapidly than a in the high subundal range, and $a_\delta/a \to \infty$ as

$$c_2/(gh)^{\frac{1}{2}} \to [1+R[(1/V^2)-1]]^{\frac{1}{2}}.$$

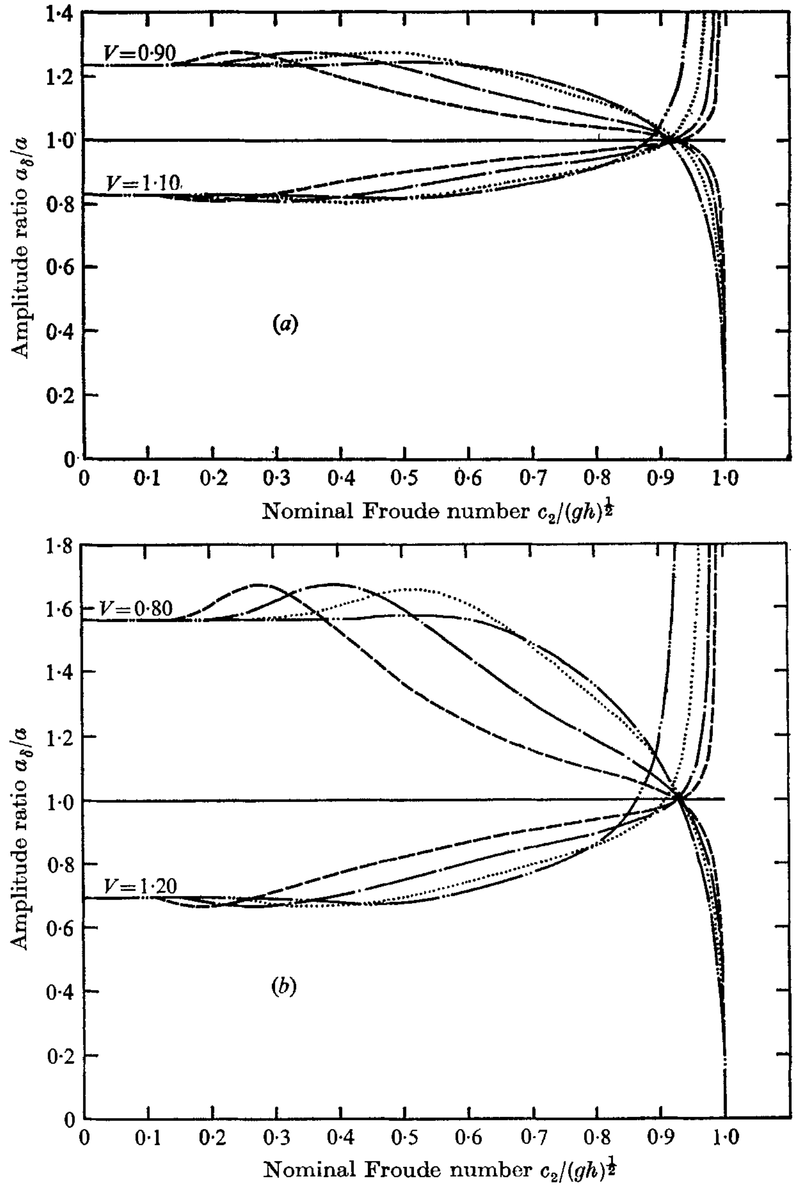

FIGURE 7. (*a*) and (*b*) The effect of the velocity defect on the amplitude of trailing waves as a function of nominal Froude number $c_2/(gh)^{\frac{1}{2}}$: ———, $V = 1$, other values of V are stated on the figures; – – – –, $R = 0{\cdot}05$; —·—·—, $R = 0{\cdot}10$; ...., $R = 0{\cdot}20$; —··—··—, $R = 0{\cdot}40$.

6. Discussion

The analysis of §§4 and 5 will only represent approximately the surface profile for the idealized hovering craft in a real situation, where the velocity profile is similar to those on figure 4. This will be particularly true of the local elevation component, since the integral in (4.3) is taken over all wave-numbers and the true equivalent uniform defect profile will depend on the wave-number. For example, the uniform velocity in the wake should be taken as the true surface velocity when k tends to infinity. However, the analysis does provide a useful method for determining the order of magnitude of the error caused by the surface wake, and hence for determining whether a stream is sufficiently uniform near the surface to be acceptable for experimental work. Similar velocity defects can also occur naturally in rivers and other open-channel flows with no upstream lid, where they are generally caused by secondary flows or wind stress. Moreover, it is always difficult to measure the velocity of water accurately near a free surface, and the analysis could be used to estimate the possible effect on waves caused by this uncertainty. For many purposes the calculations of § 3 should be sufficient.

The author would like to thank Professor J. H. Preston and Mr K. Nicholson of Liverpool University for their kindness in making available the experimental velocity profiles shown on figure 4.

REFERENCES

Binnie, A. M., Davies, P. O. A. L. & Orkney, J. C. 1955 Experiments on the flow of water from a reservoir through an open horizontal channel. I. The production of a uniform stream. *Proc. Roy. Soc.* A **230**, 225.

Hogben, N. 1967 Hovering craft over water. *Advances in Hydroscience*, **4**, 1.

Lamb, H. 1932 *Hydrodynamics*, 6th ed. Cambridge University Press.

Taylor, G. I. 1955 The action of a surface current used as a breakwater. *Proc. Roy. Soc.* A **231**, 466.